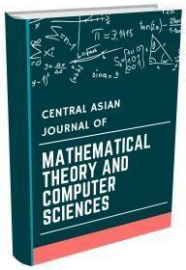

CENTRAL ASIAN JOURNAL OF MATHEMATICAL THEORY AND COMPUTER SCIENCES
https://cajmtcs.centralasianstudies.org/index.php/CAJMTCS
Volume: 05 Issue: 03 | April 2024 ISSN: 2660-5309

Article

Deep Learning Model Based Decision Support System for Kidney Cancer on Renal Images

Mustafa Asaad Hasan*[1]

1. University of Thi-Qar, Nasiriyah, Iraq
* Correspondence: Mustafa.alkhafaji@utq.edu.iq

Abstract: Kidney cancer remains one of the most lethal urological malignancies due to its lack of early symptoms and effective screening strategies. Timely diagnosis is crucial for improving treatment outcomes and patient survival. This study explores the application of deep learning models—EfficientNet-B1 and MobileNet-V2—for the classification of kidney abnormalities, including cysts, stones, tumors, and normal conditions, using computed tomography (CT) images. A dataset of 12,446 annotated kidney CT images was used for training and evaluation, with preprocessing techniques such as Gaussian filtering, Otsu's binarization, and watershed segmentation enhancing image quality. Both models were implemented and compared based on accuracy, precision, recall, F1-score, and specificity. The EfficientNet-B1 model achieved superior performance with an overall accuracy of 99.27%, demonstrating strong precision and recall across all categories. MobileNet-V2 also performed well, attaining 96.81% accuracy, though with slightly reduced precision for stone detection. The results highlight the potential of transfer learning-based CNN architectures in assisting radiologists with reliable, automated kidney disease classification, thereby contributing to earlier detection and improved patient care.

Keywords: Computational Intelligence, Nature-Inspired Algorithm, Deep Learning, Decision Support System, Kidney Cancer

Citation: Hasan, M. A. Deep learning model based decision support system for kidney cancer on renal images. Central Asian Journal of Mathematical Theory and Computer Sciences 2024, 5(3), 82-97.

Received: 14th April 2024
Revised: 14th May 2024
Accepted: 21th May 2024
Published: 28th May 2024

1. Introduction

In the kidney's, metabolized substances are filtered and eliminated from the body. In addition to regulating blood pressure, they stimulate the production of red blood cells. Around 13,000 kidney cancer cases and over 4,000 deaths were registered in 2020 due to this type of cancer, which is more prevalent among people aged 50 to 70 [1]. The most lethal type of urological cancer is kidney cancer, despite not being among the top ten prevalent oncological diseases worldwide. A lack of clear symptoms and screening tests for kidney cancer reduce the possibility of early diagnosis and effective treatment, according to [2]. In order to improve outcomes, it is essential to detect and define the disease at an early stage. By using machine learning technologies such as Convolutional Neural Networks (CNNs), medical images can be analyzed and patterns detected that would not be visible to humans[3].

It may fill the gap left by the absence of effective methods for detecting kidney cancer in its early stages [4]. Therefore, this work proposes using Convolutional Neural Networks to identify and classify kidney cancer in tomographic images. By assisting healthcare professionals in early detection of cancer, the main objective is to facilitate decision-making in individual cases, contribute to more accurate diagnoses, which may lead to more targeted and appropriate treatments for patients, which may result in better outcomes and better quality of life for them.

The kidneys not only return vitamins, amino acids, glucose, hormones, and other vital nutrients to the blood, but they also serve as filters. Among men, kidney cancer is the ninth most common cancer in the world, according to a recent study. A total of 214,000 new cases were reported by men in 2012, while 124,000 were reported by women. U.S. kidney tumors account for 3.7% of all cancers. An estimated 62,000 Americans are diagnosed with kidney cancer every year, resulting in 4,444 different types. Men are more likely to get sick than women. Several medical diagnosis tasks have shown excellent results when a Convolution Neural Network (CNN) is used [5]. The use of deep learning and machine learning models for tumor segmentation and classification is very effective. In machine learning, the learning process itself is referred to as machine learning [6]. Data processing can be accomplished by providing the appropriate data. The model performance will also be impacted by choosing the best loss function. As an example, a binary cross-entropy loss function may provide better results (losses) to classify kidney cancer.

The survival rate of bladder cancer patients in women is lower, despite being adjusted for stage at diagnosis [7],[8]. A variety of risk factors and biological mechanisms, including sex steroids, have been associated with influencing cancer development and treatment [9]. It may also be due to clinicians' varying diagnostic testing strategies that these cancers are diagnosed so quickly. The ''Be Clear on Cancer'' campaign [10], which raises public awareness of alarm symptoms like haematuria, can also be attributed to the introduction of new referral pathways, clinical guidelines, and clinical audit initiatives that have led to progressive changes in clinical practice as well. In contrast, kidney cancer is more variable in its diagnosis. The majority of diagnoses in 2015 were made via fast-track or non-fast-track routes, with 60% coming from GP referrals [11]. Approximately a fifth of kidney cancer cases are diagnosed as emergencies, compared to 18% of bladder cancer cases [12]. In most of these cancers, early detection, diagnostic testing, and referral decisions are crucial for improving the outcome [13].

In this study, EfficientNet-B1 and MobileNet-V2 model is used for kidney image classification. This involves building a web application that runs the trained model on the backend. The proposed research consists of two EfficientNet-B1 and MobileNet-V2 models which is trained using CT scan images. This article briefly describes the proposed models and their implementation, and the results are compared. Finally, the EfficientNet-B1 and MobileNet-V2 model that was trained is hosted on visual code for kidney cancer detection using a Computed Tomography (CT) scan of the image as input.

Related Work

Patients with kidney stones have been categorized based on their kidney disease using machine learning and deep learning techniques. As a way of improving diagnostic accuracy and potentially improving patient outcomes, study results are discussed. The concept of multi-classification has been applied by several authors [14] to classify renal diseases. Researchers found that 85.52 percent of kidney cysts, stones,

and tumors could be accurately identified using a pre-trained YOLOv8n-CLS model. Researchers show that deep learning models can be used to accurately classify diseases, which provides the basis for future research.

To predict the occurrence of chronic kidney disease, the author [15] proposed an ensemble model combining CNNs and LSTMs. The researchers found that combining different architectures improved each model's diagnostic capabilities, as well as its classification capabilities. In population-based studies, this method may be useful, but it cannot be used to provide personalized patient care. An author [16] categorizes CT scan images into four categories: cysts, normal states, tumors, and stones. To improve the model's capabilities, the training/testing split was 90/10, which resulted in optimal performance. The ViT model presents a modern view of kidney classification, which accurately classifies a variety of medical imaging pathologies. The authors present an automated kidney stone detection system based on CNN technology [17].

The YOLOv4 model, along with CBC preprocessing, produced an astounding accuracy rate of 96.1% for 630 DUSX images. It is important to choose the right model to ensure optimal performance as demonstrated by YOLOv4.

According to the authors [18], EGFR-sensitizing mutations in non-small cell lung cancer (NSCLC) exhibit shallow and deep combination features. They have developed a fusion model that is more accurate at identifying cancer mutations for personalized cancer treatment. NESICH (Neuroendoscopic Parafascicular Evacuation of Spontaneous Intracerebral Hemorrhage) is effective in removing spontaneous intracerebral hemorrhages, according to the Author [19]. In the treatment of ICH, preliminary results of a multicenter study are promising. In this study [20], screening methods for PA were compared in patients taking medications that interfere with their health. An analysis of the microbiota of patients with peritoneal fibrosis on peritoneal dialysis [21] was conducted. There is a link between the peritoneal microbiota composition and dialysis-related issues, according to their findings. An endovascular localization and biopsy system for pulmonary lesions was presented by the author [22]. A trend in medical procedures is using robotics to improve accuracy and accessibility, such as lung cancer diagnosis. During spontaneous intracerebral hemorrhage (ICH), the author [23] described an image-guided paracortical spinal tract approach. Using image-guided neurosurgical interventions can maximize patient outcomes and minimize brain damage in this method of neurosurgery.

By improving diagnostic accuracy and efficiency through prediction and detection, machine learning and deep learning algorithms are receiving increasing attention. A number of studies have searched and showed diverse machine learning techniques that could optimize the prediction and detection of CKD, with each adding a piece to the development of non-invasive diagnostic tools. CKD was identified using random forest, support vector machines, and artificial neural networks in the work of [24]. A Random Forest and ANN model performed better than other classifiers based on the results. A critical part of improving CKD diagnosis is to choose the right algorithm, and among them, tree-based models have some advantages in dealing with complex datasets. Additionally, the study showed that features can be selected more effectively and preprocessing techniques can be optimized to improve performance. Researchers have reported significant improvement in early disease detection in various studies, such as that of [25], which used logistic regression and SVM in developing predictors of CKD. Model accuracy improvements were explored with feature engineering and hyperparameter tuning. According to them, successful prediction of CKD depends significantly on the quality of the input features, which

should include clinical as well as demographic information. Combining multiple algorithms, this work identified a possible hybrid approach for improving diagnostic accuracy and reducing false-positive results. Using machine learning techniques, the author [26] investigated the CKD prediction. Health-care applications must be interpretable, they pointed out. According to their study, Decision Trees and Gradient Boosting Machines were incredibly accurate at predicting CKD. A second point discussed by the authors was that since all models are fundamentally a balance between their complexity and their interpretability, deep neural network complex models may also provide clinically acceptable performance, but explainability is one of the biggest concerns in clinical settings. Furthermore, this study emphasized the importance of developing hybrid models in such a way that their performance and interpretability are maximized. Table 1 shows the existing model analysis based on accuracy and research gaps.

The transfer of knowledge has also contributed significantly to the diagnosis of kidney disease. An article [27] found nephrolithiasis (kidney stones) by cascading CNNs. By adding normalization and segmentation to the model, they improved its performance. To find kidney tumors, we trained and fine-tuned the EfficientNetB0 models. Model development was made quick and accurate with transfer learning. Also applied XResNet-50 for the detection and localization of kidney stones in addition to these architectures. They achieved impressive performance in kidney regions using targeted segmentation (95% sensitivity, 97% precision).

Table 1. Comparative result analysis based on existing state-of-art.

Reference	Model	Accuracy	Research Gaps
[28]	EfficientNetB0	96%	Potentially generalizable in resource-limited environments
[29]	EfficientNetB0	94%	The information provided for common kidney conditions is detailed, but insights into rare kidney conditions are lacking.
[30]	CNN Models	91%	Low generalization is associated with mixed imaging modalities
[31]	Vision Transformer (ViT)	92%	Datasets that are small and noisy are suboptimal
[32]	Vision Transformer (ViT) for cysts/tumors	93%	Needs hybrid addition with CNNs
[33]	XResNet-50	97%	The precision is high, but the interpretability needs to be advanced.
[34]	EfficientNetB0	89%	Lacks global dataset validation
[35]	SVM with preprocessing techniques	98%	Aims to remove noise, but lacks generalization.
[36]	Optimized ANN (Crow Search Algorithm)	High	Focus on small datasets; no exploration of recent deep learning techniques
[37]	Diverse kidney datasets	85%	Lack of labeled rare disease data.

2. Materials and Methods

Aiming to identify kidney disease from CT scan images, this research evaluated the effectiveness of various deep-learning models. Due to its flexibility, cost-effectiveness, and consistency in planning and executing projects, the approach is widely used. The Figure 1 shows the systematic block diagram of the proposed methodology.

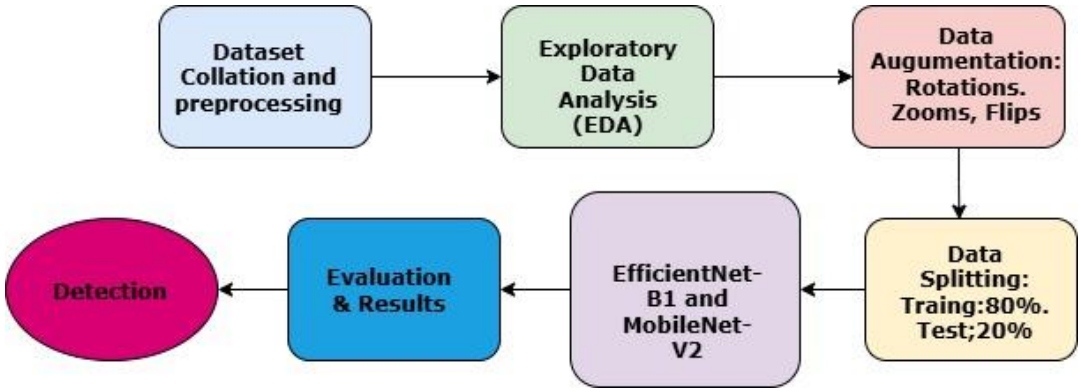

Figure 1. The proposed methodology.

Dataset

This study used a second dataset on the Kaggle platform called CT Kidney Dataset: Normal Cyst Tumor and Stone [38]. A variety of hospitals in Dhaka, Bangladesh, used Picture Archiving and Communication Systems (PACS) to collect the pictures. Images depict kidney tumors, cysts, normal kidney structures, or kidney stones, all of which are diagnosed in patients. A contrast-enhanced CT section as well as a non-contrast CT section of the abdomen and program was selected in accordance with imaging protocols. Several diagnostic categories were carefully curated, anatomical regions were segmented, and patient metadata and information were removed before each DICOM scan was anonymized. After being converted to .jpg format, the images were resized. The images were independently verified by radiologists and medical technologists. Figure 2 illustrates the few sample of the proposed dataset.

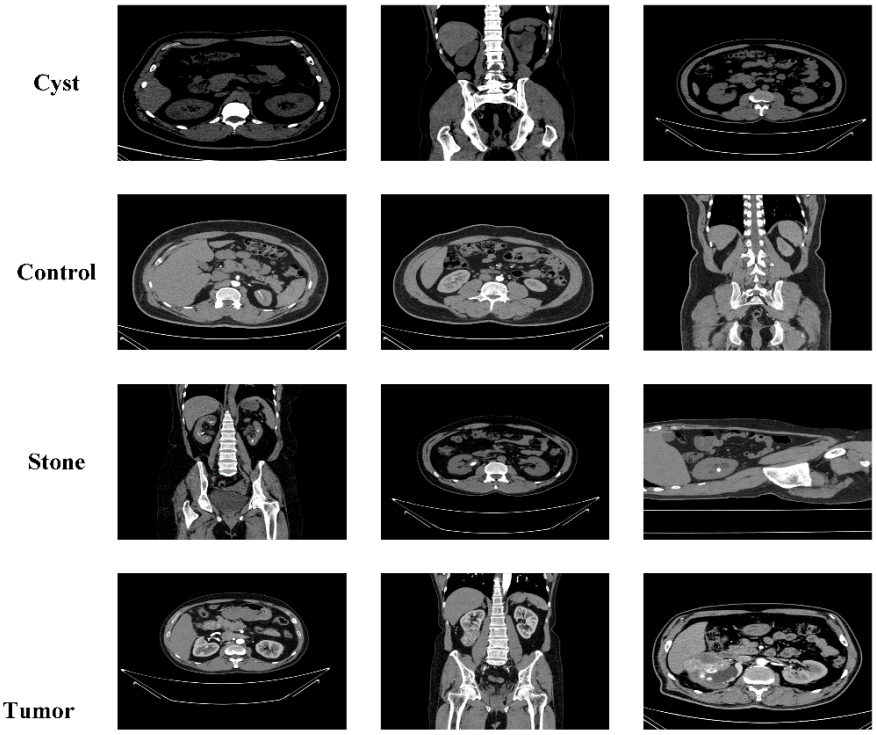

Figure 2. Sample images from the Dataset.

This dataset contains a total of 12,446 images, 3709 represent cysts, 5077 represent normal images, 1377 represent stones, and 2283 represent tumors as shown in Figure 3. Due to the model's rich and diverse structure, it can differentiate between different kidney lesions.

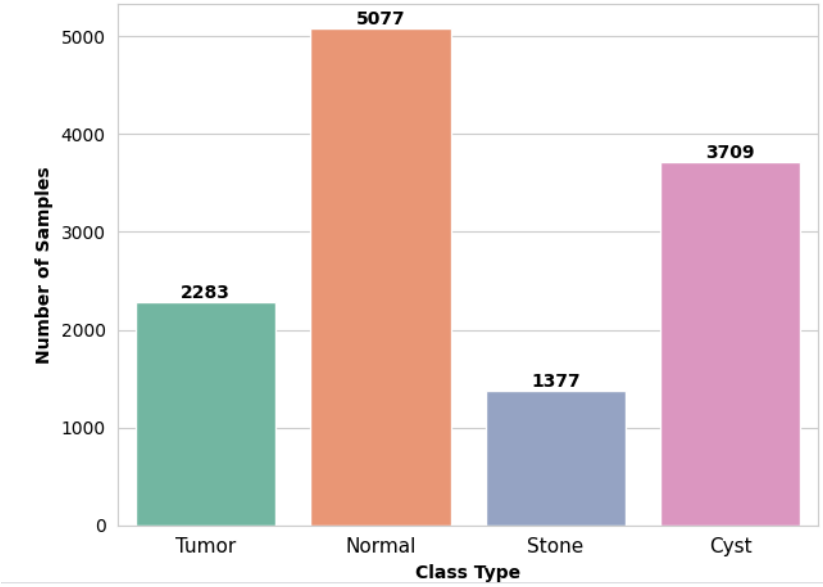

Figure 3. Distribution of the dataset into Tumor, normal, stone and cyst.

The two image transformation is measured by PyTorch library. As part of the training transform, several random augmentations are applied, including resizing, flipping, rotating, and applying affine transformations. Testing transforms only resize and convert images to tensors to ensure consistent evaluation. According to figure 4, both resize images to 128x128 pixels and convert them to tensor format as input for models.

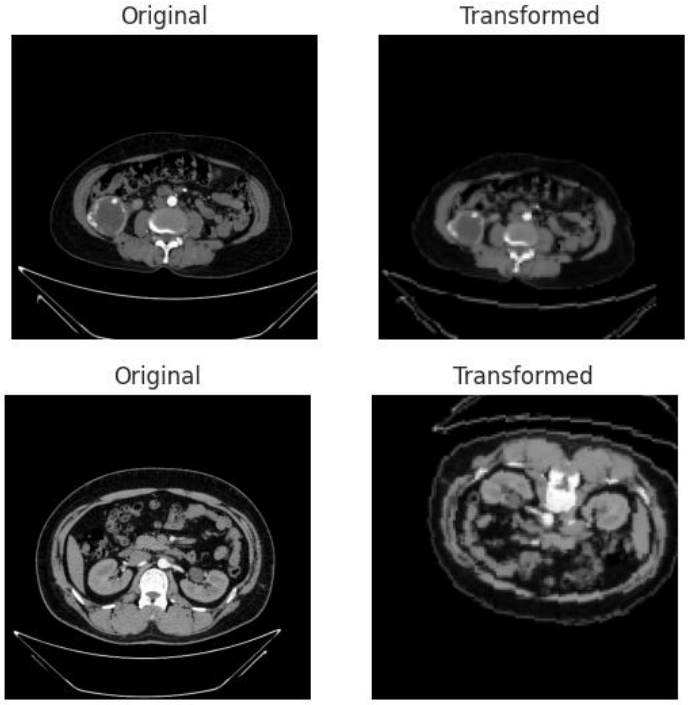

Figure 4. Sample images of the image transformation.

Data Preprocessing

Utilizing the most efficient noise reduction technique is crucial to improving the quality of input data. Gaussian filters can be used as an example. By reducing high-frequency noise and details, the Gaussian filter is an important tool for improving the model's accuracy. The 2D Gaussian kernel (x,y,σ) is mathematically convolved with the original image I(x,y), where _ represents the standard deviation. Eq. (1) defines convolution as follows:

$$I_{smoothed}(x,y) = \sum_{i=-\infty}^{\infty} \sum_{i=-\infty}^{\infty} I(x-i, y-j)\, XG(i,j,\sigma \quad (1)$$

The Gaussian function (x, y, σ) , is given by Eqn. (2):

$$G(x,y,\sigma) = \frac{1}{2\pi\sigma^{2^e}} - (x^2+y^2)/(2\sigma^2) \quad (2)$$

A kernel coordinate is represented by the x-plane, and a Gaussian distribution spread is represented by the y-plane.

Image Segmentation

Image segmentation is an important task when dealing with computer vision, especially when detecting and classifying objects.

With Otsu's binarization, grayscale images can be automatically segmented into foregrounds and backgrounds by using threshold values. In this method of segmentation, grayscale images are converted into binary images, which show cysts, stones, or tumors as foreground objects and the background is removed. Otsu's binarization states that thresholds that minimize intra-class variance maximize inter-class variance. Eqn. (3) in Otsu's method calculates the between-class variance ($\sigma^2 B$) as follows:

$$\sigma_B^2(t) = w1(t) X_{w2}(t) X[\mu_1(t) - \mu_2(t)]^2 \quad (3)$$

Specifically, $w1(t)w2(t)$ represents the probability of pixels being classified as background or foreground, and $\mu_1(t) - \mu_2(t)$ represents the average intensity of pixels in the two categories.

Transforms based on distance calculate the distance between pixels that fall within each pixel's nearest boundary in an image. The kidney region's boundary is identified using distance transform during kidney image segmentation. Based on the distance between an image's pixels and its nearest border, we can use the distance transform to assign a value to each pixel. There is a difference between a pixel close to the boundary and a pixel farther away from the boundary in terms of distance value. Using the Euclidean distance metric as a basis, Eqn. (4) can be used to transform distances:

$$D(x,y) = \sqrt{\sum_{i=-k}^{K} \sum_{j=-k}^{K} I(x+i, y+j)\, XI(x+i, y+j)} \quad (4)$$

The original image shows $D(x,y)$as the distance between pixels, $(x,y), I(x + I, y+j)$ as the intensity of the pixel at coordinate $(x+I, y+j)$,, and k as the area around each pixel.

Watershed transforms are effective in various biomedical imaging applications for separating objects from backgrounds. Pixel intensities are treated as

topographical heights in the watershed transform for grayscale images. Images are treated as topographic landscapes, with intensity values representing the landscape's height. Different regions are separated by watershed lines according to the topology of the landscape. A mathematical description of the watershed transformation can be obtained by using morphological reconstruction and flooding. A simplified description of the watershed transform equation is given below in the context of grayscale images (Eqn. 5):

$$W = Imposed\ Markers \oplus Regional\ Minima\ (Gradient\ Image) \quad (5)$$

Watershed transformations result in W, imposed markers are placed on the image, gradient images are the original grayscale gradients, and morphological reconstruction is the fundamental operation.

Training Model Architecture

EfficientNet-B1 Model: The transfer learning model of EfficientNet-B1 [39] has shown outstanding performance in image classification tasks. It is a major advance in deep learning. Researchers at Google developed EfficientNet-B1, a neural network design that is both compact and scalable. By combining these techniques, we have been able to achieve impressive accuracy with fewer parameters. Through the novel compound scaling approach of this architecture, the depth, width, and resolution of the network are uniformly scaled. Thus, it can adapt to a variety of datasets and processing resources. Object detection, medical imaging, and other computer vision applications can benefit from the use of the EfficientNet-B1. Because it uses pre-trained information from large-scale datasets, the layered system is popular. In the current research, we are using the EfficientNet-B1 transfer learning model. It consists of the following layers:

Batch Normalization Layer: Activations in this normalization layer are normalized based on the mini-batch, which facilitates increased training speed and stability. In addition to accelerated training and better generalization performance, reduced internal covariate shift is one aspect of taking out the mean of a mini-batch and dividing it by standard deviation.

Dense Layer: In the neural network architecture, a dense layer, or fully connected layer, is a layer where each neuron serves as one unit. A linear transformation is performed on the input items before they are passed through the activation function. There are 256 neurons in this dense layer.

Dropout Layer: To address over fitting in neural networks, the dropout layer is used. The dropout rate in this model is 0.4.

Output Layer: There are four neurons in this layer, each representing one of four classes: cyst, normal, stone, and tumor.

MobileNetV2 Model: On-device vision has been significantly advanced by convolutional neural networks. In order to achieve MobileNetV2's efficiency, depth-wise separable convolutions are used. In contrast to traditional convolutions, the model breaks them down into depth-wise and point-wise convolutions to reduce computation complexity while maintaining the network's ability to capture difficult features [40]. Inverted residuals are used in MobileNetV2 to further improve its performance by applying depth-wise separable convolutions, then projecting to a lower-dimensional space. For real-time data applications, MobileNetV2's integrated architecture ensures high accuracy in detecting objects and classifying images. It

requires minimal memory and maintains low latency. It is particularly useful with regards to ovarian cancer and identifying normal glomeruli [41], which require precise image analysis. MobileNetV2, which is a depth-wise separable convolution, can be represented as follows:

$$Y = PWConv2D(DWConv2D(X)) \quad (6)$$

MobileNetV2's linear bottleneck layer looks like this:

$$Y = PWConv2D(DWConv2D\big(D(X)\big) + X \quad (7)$$

PWConv2D represents the point wise convolution, while DWConv2D represents the depth wise separable convolution. Training gradients are helped by the addition of X, which establishes a residual connection.

3. Results and Discussion

A Windows 10 workstation equipped with an Intel Core i7-8700 processor, 16 GB of RAM, and an Nvidia GeForce 4GB graphics card was used to evaluate the methods and compare them with comparative models. Python 3.8 was used to implement all models, as well as Keras and Tensor Flow libraries for training and executing networks. Model performance is measured using the metrics Recall (Re), F1-Score (F1), Precision (Pr), and Accuracy (Acc). In equations (8) to (11), performance metrics are presented.

$$P_r = \frac{TP}{TP+FP} \quad (8)$$

$$R_e = \frac{TP}{TP+FN} \quad (9)$$

$$F_1 = 2.\frac{P_r x R_e}{P_r + R_e} \quad (10)$$

$$A_{cc} = \frac{TP+TN}{TP+TN+FP+FN} \quad (11)$$

True positives are TP, true negatives are TN, false positives are FP, and false negatives are FN.

The EfficientNet-B1 model's performance on the CT kidney dataset is presented in Table 2 and Figure 5, which presents key metrics for each class and an overall average. In terms of accuracy, the model was able to correctly classify kidney conditions with an average accuracy of 99.27%. The specificity of the model, which measures how often negatives are correctly identified, averaged 100%, suggesting it seldom produces false positives. The precision, or the percentage of correct positive identifications, averaged 95.13%. A high recall of 97.84% was recorded, which is the proportion of true positives correctly identified. In terms of precision and recall, the F1 Score averaged 96.13%, indicating a good balance between the two.

Table 2. The results of EfficientNet-B1 evaluated on the CT kidney dataset.

Class	Accuracy (%)	Specificity (%)	Precision (%)	Recall (%)	F1 Score (%)
Cyst	98.84	100.00	100.00	93.65	97.10
Normal	99.65	100.00	99.87	98.71	99.29
Stone	98.09	97.77	79.53	100.00	88.86
Tumor	100.00	100.00	100.00	98.28	99.28
Average	99.27	100.00	95.13	97.84	96.13

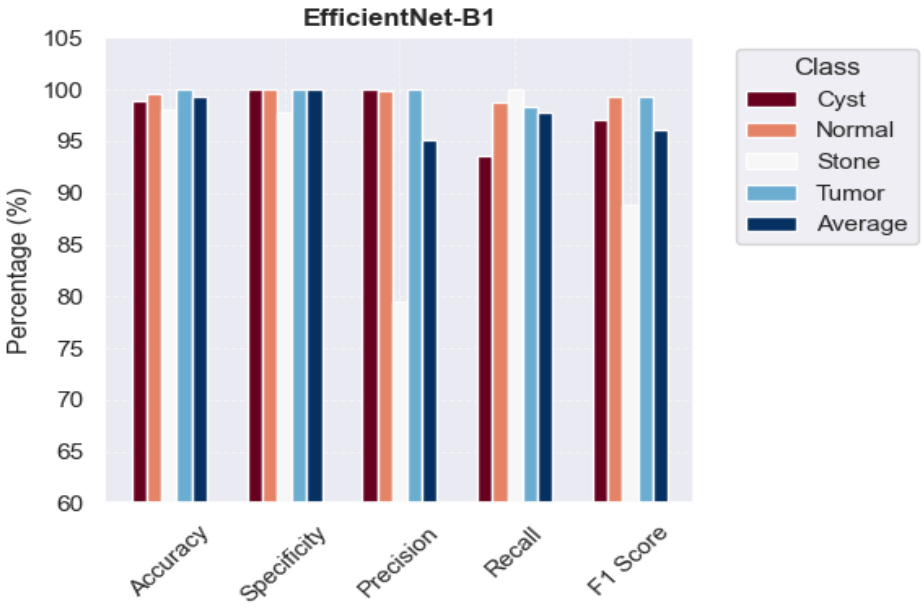

Figure 5. Performance analysis of EfficientNet-B1 based on the dataset classes.

MobileNetV2 showed excellent performance across a wide range of metrics using based on CT kidney data. Averaging 96.81 percent accuracy, 98.08% specificity, 92.23% precision, 94.96% recall, and 93.71% F1 score, the model achieved an average of 95.81 percent accuracy, 98.08% specificity, 92.23% precision, and 94.21% recall as shown in Figure 6 and Table 3. A high recall (97.36%) was found for the 'Normal' and 'Tumor' classes, respectively, while a low precision (75.85%) was observed for the 'Stone' class, suggesting a considerable number of false positives. Cyst performed well with a 94.05% F1 Score.

Table 3. The results of MobileNetV2 evaluated on the CT kidney dataset.

Class	Accuracy (%)	Specificity (%)	Precision (%)	Recall (%)	F1 Score (%)
Cyst	96.45	98.92	97.53	90.82	94.05
Normal	97.80	99.00	97.20	96.45	96.82
Stone	95.10	95.65	75.85	97.36	85.24
Tumor	97.90	98.75	98.32	95.22	96.74
Average	96.81	98.08	92.23	94.96	93.71

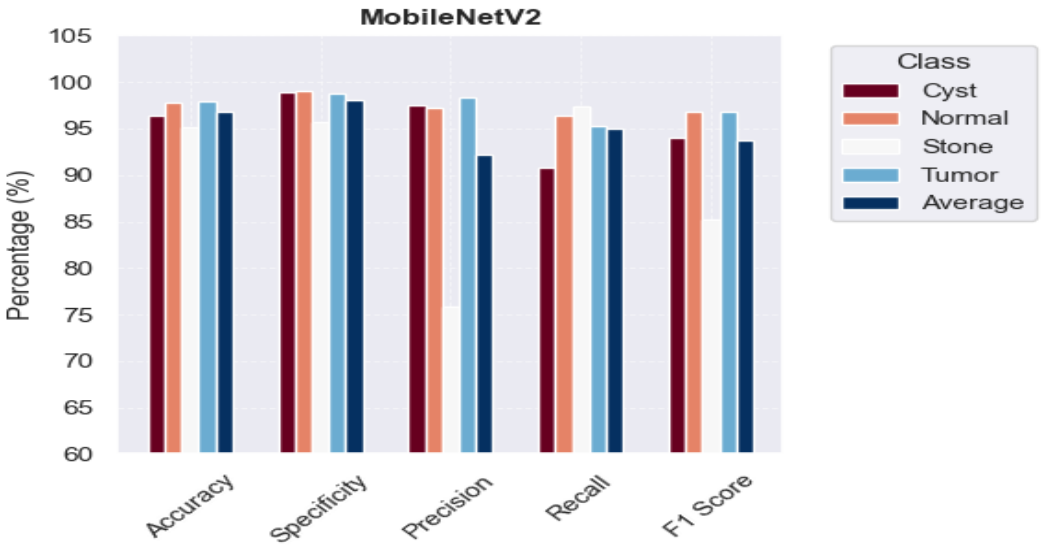

Figure 6. Performance analysis of MobileNet-B1 based on the dataset classes.

Figure 7 & 8 shows the confusion matrices of EfficientNet-B1, and MobileNetV2 when tested on the CT kidney dataset for the four classes: cyst, normal, stone, and tumor. The test set of the CT kidney has 3709 image for cysts, 5077 represent normal images, 1377 represent stones, and 2283 represent tumors. The MobileNetV2 model correctly identified and achieves a 96.81% accuracy rate. There were two cases where cyst samples were incorrectly identified as stones and labeled as FN. This confusion arose due to overlapping features in imaging; both conditions can appear as dense, rounded areas in scans. The model may find it challenging to differentiate between these conditions in borderline scenarios.

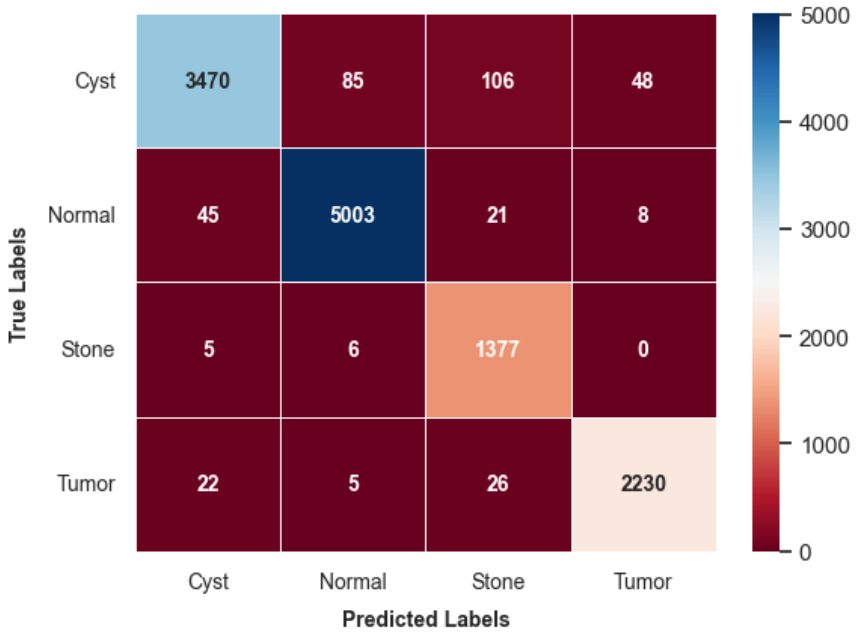

Figure 7. Performance analysis according to confusion metric of EfficientNet-B1 model.

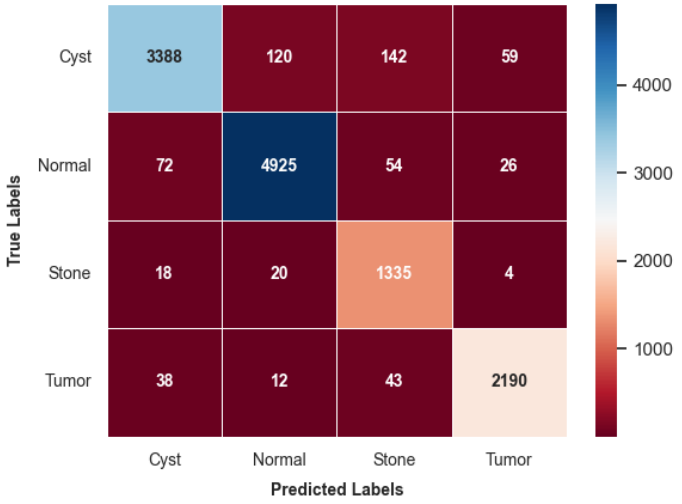

Figure 8. Performance analysis according to confusion metric of MobileNetV2 model.

Classification reports are shown in this work for EfficientNet-B1 and MobileNet-V2, which eliminate their performances across the four classes: Tumor, Cyst, Normal, and Stone. EfficientNet-B1 has generally achieved an overall accuracy of 99.27% with very strong precision and recall across all classes, especially Tumor and Cyst with F1-scores of 100%. The macro-average F1-score of EfficientNet-B1 is 95.13 while its weighted average F1-score is 96.13, showing that this network performs balanced among the different classes. MobileNet-V2 had a much overall lower performance, with an overall accuracy of 96.81%. While it shared a similarly high performance on the Tumor and Cyst classes with scores of 96.74 and 94.05 F1-score respectively, its performance was notably on the Normal class is 96.82 generally performed better and had generalized well across all classes, as illustrated in Figure 9.

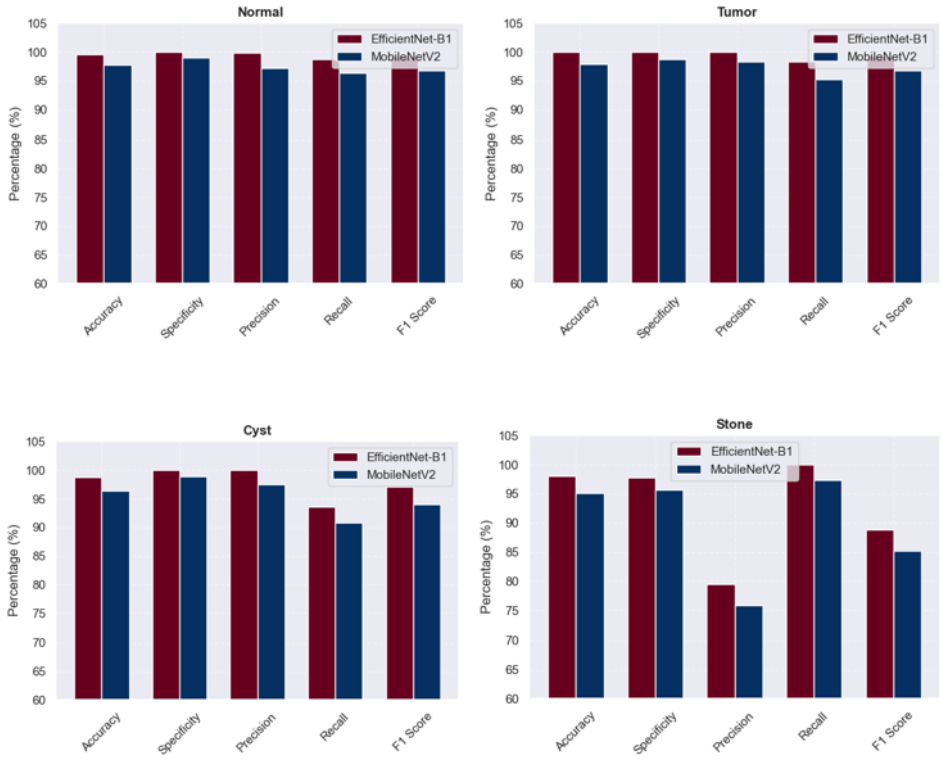

Figure 9. Classification report analysis of EfficientNet-B1 and MobileNet-V2 model.

4. Conclusion

This study demonstrates the effectiveness of deep learning models in classifying kidney diseases using CT scan images. The EfficientNet-B1 model outperformed MobileNet-V2, achieving 99.27% overall accuracy and near-perfect specificity, making it highly reliable for clinical applications. MobileNet-V2, while slightly less accurate, offers advantages in computational efficiency and suitability for real-time applications. These findings confirm that convolutional neural network-based transfer learning approaches can significantly enhance diagnostic accuracy, reduce human error, and support medical professionals in early detection of kidney abnormalities. Future work will focus on integrating hybrid deep learning frameworks, improving interpretability for clinical adoption, and expanding validation across diverse datasets and imaging modalities.

REFERENCES

[1] I. Corporativa and M. Roman–mariana, "BAVENCIO® combinado com Inlyta® para carcinoma de células renais avançado tem resultados positivos em estudo fase III," *CEP*, vol. 4578, p. 000, 2018.

[2] V. Meireles Pereira Santos, A. C. Patrocinio, W. Chaves De Souza Carvalho, and P. M. De Sousa, "Renal Cancer Classification in Tomographic Images Using Convolutional Neural Networks to Assist Early Diagnosis," *Rev. Informática Teórica E Apl.*, vol. 32, no. 1, pp. 61–66, Feb. 2025, doi: 10.22456/2175-2745.143539.

[3] S. Verma *et al.*, "An automated face mask detection system using transfer learning based neural network to preventing viral infection," *Expert Syst.*, p. e13507, 2024.

[4] D. Alzu'bi *et al.*, "Kidney Tumor Detection and Classification Based on Deep Learning Approaches: A New Dataset in CT Scans," *J. Healthc. Eng.*, vol. 2022, pp. 1–22, Oct. 2022, doi: 10.1155/2022/3861161.

[5] P. Rani, S. Verma, S. P. Yadav, B. K. Rai, M. S. Naruka, and D. Kumar, "Simulation of the lightweight blockchain technique based on privacy and security for healthcare data for the cloud system," *Int. J. E-Health Med. Commun. IJEHMC*, vol. 13, no. 4, pp. 1–15, 2022.

[6] S. Kollem, C. R. Prasad, J. Ajayan, V. Malathy, and A. Subbarao, "Brain tumor MRI image segmentation using an optimized multi-kernel FCM method with a pre-processing stage," *Multimed. Tools Appl.*, vol. 82, no. 14, pp. 20741–20770, June 2023, doi: 10.1007/s11042-022-14045-x.

[7] J. A. Cohn, B. Vekhter, C. Lyttle, G. D. Steinberg, and M. C. Large, "Sex disparities in diagnosis of bladder cancer after initial presentation with hematuria: A nationwide claims-based investigation," *Cancer*, vol. 120, no. 4, pp. 555–561, Feb. 2014, doi: 10.1002/cncr.28416.

[8] G. Lyratzopoulos, R. D. Neal, J. M. Barbiere, G. P. Rubin, and G. A. Abel, "Variation in number of general practitioner consultations before hospital referral for cancer: findings from the 2010 National Cancer Patient Experience Survey in England," *Lancet Oncol.*, vol. 13, no. 4, pp. 353–365, Apr. 2012, doi: 10.1016/S1470-2045(12)70041-4.

[9] J. Dobruch *et al.*, "Gender and Bladder Cancer: A Collaborative Review of Etiology, Biology, and Outcomes," *Eur. Urol.*, vol. 69, no. 2, pp. 300–310, Feb. 2016, doi: 10.1016/j.eururo.2015.08.037.

[10] "Be Clear on Cancer", [Online]. Available: https://www.cancerresearchuk.org/health-professional/awareness-and-prevention/be-clear-on-cancer

[11] T. A. Ellison, "Economic evaluation in kidney transplantation," PhD Thesis, Johns Hopkins University, 2015. Accessed: Oct. 05, 2025. [Online]. Available: https://jscholarship.library.jhu.edu/items/6a58c31a-3e19-4ac0-8ca4-e64ab0168a37

[12] Y. Zhou *et al.*, "Diagnosis of cancer as an emergency: a critical review of current evidence," *Nat. Rev. Clin. Oncol.*, vol. 14, no. 1, pp. 45–56, Jan. 2017, doi: 10.1038/nrclinonc.2016.155.

[13] R. D. Neal *et al.*, "Is increased time to diagnosis and treatment in symptomatic cancer associated with poorer outcomes? Systematic review," *Br. J. Cancer*, vol. 112, no. S1, pp. S92–S107, Mar. 2015, doi: 10.1038/bjc.2015.48.

[14] S. D. Pande and R. Agarwal, "Multi-Class Kidney Abnormalities Detecting Novel System Through Computed Tomography," *IEEE Access*, vol. 12, pp. 21147–21155, 2024, doi: 10.1109/ACCESS.2024.3351181.

[15] D. Saif, A. M. Sarhan, and N. M. Elshennawy, "Deep-kidney: an effective deep learning framework for chronic kidney disease prediction," *Health Inf. Sci. Syst.*, vol. 12, no. 1, p. 3, Dec. 2023, doi: 10.1007/s13755-023-00261-8.

[16] R. Subedi, S. Timilsina, and S. Adhikari, "Kidney CT Scan Image Classification Using Modified Vision Transformer," *J. Eng. Sci.*, vol. 2, no. 1, pp. 24–29, Dec. 2023, doi: 10.3126/jes2.v2i1.60381.

[17] U. Kilic, I. Karabey Aksakalli, G. Tumuklu Ozyer, T. Aksakalli, B. Ozyer, and S. Adanur, "Exploring the Effect of Image Enhancement Techniques with Deep Neural Networks on Direct Urinary System X-Ray (DUSX) Images for Automated Kidney Stone Detection," *Int. J. Intell. Syst.*, vol. 2023, no. 1, p. 3801485, Jan. 2023, doi: 10.1155/2023/3801485.

[18] X. Yao *et al.*, "Fusion of shallow and deep features from 18F-FDG PET/CT for predicting EGFR-sensitizing mutations in non-small cell lung cancer," *Quant. Imaging Med. Surg.*, vol. 14, no. 8, pp. 5460–5472, Aug. 2024, doi: 10.21037/qims-23-1028.

[19] L. Wang *et al.*, "Neuroendoscopic Parafascicular Evacuation of Spontaneous Intracerebral Hemorrhage (NESICH Technique): A Multicenter Technical Experience with Preliminary Findings," *Neurol. Ther.*, vol. 13, no. 4, pp. 1259–1271, Aug. 2024, doi: 10.1007/s40120-024-00642-5.

[20] X. Li *et al.*, "TLDA: A transfer learning based dual-augmentation strategy for traditional Chinese Medicine syndrome differentiation in rare disease," *Comput. Biol. Med.*, vol. 169, p. 107808, Feb. 2024, doi: 10.1016/j.compbiomed.2023.107808.

[21] J. Fan *et al.*, "Comparative analysis of gut microbiota in incident and prevalent peritoneal dialysis patients with peritoneal fibrosis, correlations with peritoneal equilibration test data in the peritoneal fibrosis cohort," *Ther. Apher. Dial.*, pp. 1744-9987.14226, Nov. 2024, doi: 10.1111/1744-9987.14226.

[22] X. Duan *et al.*, "A Novel Robotic Bronchoscope System for Navigation and Biopsy of Pulmonary Lesions," *Cyborg Bionic Syst.*, vol. 4, p. 0013, Jan. 2023, doi: 10.34133/cbsystems.0013.

[23] C. Zhang *et al.*, "Hematoma Evacuation via Image-Guided Para-Corticospinal Tract Approach in Patients with Spontaneous Intracerebral Hemorrhage," *Neurol. Ther.*, vol. 10, no. 2, pp. 1001–1013, Dec. 2021, doi: 10.1007/s40120-021-00279-8.

[24] M. M. Nishat *et al.*, "A Comprehensive Analysis on Detecting Chronic Kidney Disease by Employing Machine Learning Algorithms.," *EAI Endorsed Trans. Pervasive Health Technol.*, vol. 7, no. 29, 2021, Accessed: Oct.05,2025.[Online].Available: https://pdfs.semanticscholar.org/3e23/7ace3594a64028fa3eeac24bef98b56ae093.pdf

[25] D. A. Debal and T. M. Sitote, "Chronic kidney disease prediction using machine learning techniques," *J. Big Data*, vol. 9, no. 1, p. 109, Nov. 2022, doi: 10.1186/s40537-022-00657-5.

[26] P. Chittora *et al.*, "Prediction of Chronic Kidney Disease - A Machine Learning Perspective," *IEEE Access*, vol. 9, pp. 17312–17334, 2021, doi: 10.1109/ACCESS.2021.3053763.

[27] H. Panwar, P. K. Gupta, M. K. Siddiqui, R. Morales-Menendez, P. Bhardwaj, and V. Singh, "A deep learning and grad-CAM based color visualization approach for fast detection of COVID-19 cases using chest X-ray

and CT-Scan images," *Chaos Solitons Fractals*, vol. 140, p. 110190, Nov. 2020, doi: 10.1016/j.chaos.2020.110190.

[28] D. A. Salokhe, "Study of Deep Learning Models for Kidney Disease Classification Using CT Images," PhD Thesis, Dublin, National College of Ireland, 2024. Accessed: Oct. 05, 2025. [Online]. Available: https://norma.ncirl.ie/8792/

[29] G. Kaur, N. Sharma, S. Malhotra, S. Devliyal, and R. Gupta, "Advancements in Chronic Kidney Disease Diagnosis: Leveraging EfficientNetB3 for Accurate CT Image Classification," in *2024 Asia Pacific Conference on Innovation in Technology (APCIT)*, MYSORE, India: IEEE, July 2024, pp. 1–6. doi: 10.1109/APCIT62007.2024.10673696.

[30] S. N. Almuayqil, S. Abd El-Ghany, A. A. Abd El-Aziz, and M. Elmogy, "KidneyNet: A Novel CNN-Based Technique for the Automated Diagnosis of Chronic Kidney Diseases from CT Scans," *Electronics*, vol. 13, no. 24, p. 4981, Dec. 2024, doi: 10.3390/electronics13244981.

[31] S. Aburass, O. Dorgham, J. Al Shaqsi, M. Abu Rumman, and O. Al-Kadi, "Vision Transformers in Medical Imaging: a Comprehensive Review of Advancements and Applications Across Multiple Diseases," *J. Imaging Inform. Med.*, Mar. 2025, doi: 10.1007/s10278-025-01481-y.

[32] M. Saraei, M. Lalinia, and E.-J. Lee, "Deep Learning-Based Medical Object Detection: A Survey," *IEEE Access*, vol. 13, pp. 53019–53038, 2025, doi: 10.1109/ACCESS.2025.3553087.

[33] K. Yildirim, P. G. Bozdag, M. Talo, O. Yildirim, M. Karabatak, and U. R. Acharya, "Deep learning model for automated kidney stone detection using coronal CT images," *Comput. Biol. Med.*, vol. 135, p. 104569, Aug. 2021, doi: 10.1016/j.compbiomed.2021.104569.

[34] Y. Kumar, T. P. S. Brar, C. Kaur, and C. Singh, "A Comprehensive Study of Deep Learning Methods for Kidney Tumor, Cyst, and Stone Diagnostics and Detection Using CT Images," *Arch. Comput. Methods Eng.*, May 2024, doi: 10.1007/s11831-024-10112-8.

[35] R. Ahmad and B. Mohanty, "A novel computing scheme based on pattern matching for identification of nephron loss and chronic kidney disease stage," *Turk. J. Electr. Eng. Comput. Sci.*, vol. 31, no. 7, pp. 1237–1254, Nov. 2023, doi: 10.55730/1300-0632.4045.

[36] N. Vasudeva, V. S. Dhaka, and D. Sinwar, "Enhancing kidney stone diagnosis with AI-driven radiographic imaging: a review," *Discov. Artif. Intell.*, vol. 5, no. 1, p. 200, Aug. 2025, doi: 10.1007/s44163-025-00434-2.

[37] S. Elbedwehy, E. Hassan, A. Saber, and R. Elmonier, "Integrating neural networks with advanced optimization techniques for accurate kidney disease diagnosis," *Sci. Rep.*, vol. 14, no. 1, p. 21740, Sept. 2024, doi: 10.1038/s41598-024-71410-6.

[38] M. N. Islam, M. Hasan, Md. K. Hossain, Md. G. R. Alam, M. Z. Uddin, and A. Soylu, "Vision transformer and explainable transfer learning models for auto detection of kidney cyst, stone and tumor from CT-radiography," *Sci. Rep.*, vol. 12, no. 1, p. 11440, July 2022, doi: 10.1038/s41598-022-15634-4.

[39] A. Kumar and N. Sharma, "Detection and Classification of Oral Cancer Using Machine Learning Models," in *2023 3rd International Conference on Technological Advancements in Computational Sciences (ICTACS)*, Tashkent, Uzbekistan: IEEE, Nov. 2023, pp. 522–528. doi: 10.1109/ICTACS59847.2023.10390071.

[40] S. H. Kassani, P. H. Kassani, M. J. Wesolowski, K. A. Schneider, and R. Deters, "Classification of Histopathological Biopsy Images Using Ensemble of Deep Learning Networks," 2019, *arXiv*. doi: 10.48550/ARXIV.1909.11870.

[41] M. Robin, A. Ravikumar, and J. John, "Classification of Histopathological Breast Cancer Images using Pretrained Models and Transfer Learning," in *Congress on Intelligent Systems*, vol. 111, M. Saraswat, H. Sharma, K. Balachandran, J. H. Kim, and J. C. Bansal, Eds., in Lecture Notes on Data Engineering and

Communications Technologies, vol. 111. , Singapore: Springer Nature Singapore, 2022, pp. 587–597. doi: 10.1007/978-981-16-9113-3_43.